Indian Journal of Science and Technology Vol.2 No. 10 (Oct 2009) ISSN: 0974- 6846

Temperature and doping dependencies of hot electron transport properties in bulk GaP, InP and $Ga_{0.5}In_{0.5}P$

A. Mokhles Gerami[1], H.Rahimpour Soleimani[1], H. Arabshahi[2], and M. R. Khalvati[3]
[1]*Dept. of Physics, Univ. of Guilan, Rasht, Iran;* [2] *Dept. of Physics, Ferdowsi Univ. of Mashhad, Mashhad, Iran*
[3] *Department of physics, Shahrood University of Technology, Shahrood, Iran*
arabshahi@um.ac.ir

Abstract: An ensemble Monte Carlo simulation has been carriedout to study electron transport properties in GaP, InP and $Ga_{0.5}In_{0.5}P$ materials. The simulation results show that intervalley electron transfer plays a dominant role in higher electric fields leading to a strongly inverted electron distribution and to a large negative differential conductance. In addition, the electron velocity in GaP is less sensitive to temperature than other group III-V semiconductors like InP and $Ga_{0.5}In_{0.5}P$. So GaP devices are expected to be more tolerant to self-heating and high ambient temperature device modeling.

Keywords: Ensemble Monte Carlo; polar optical phonons; deformation potential; self-heating.

Introduction

The study of electron transport in semiconductors at high electric fields has reached an important stage in the last few years. Nowadays the microscopic transport model based on the Monte Carlo method seems to be adequate for studying of electronic transports characteristic in bulk and semiconductor devices (Fischetti & Laux, 1991). In this paper we deal with electron transport in bulk of GaP, InP and $Ga_{0.5}In_{0.5}P$ which can used in design and analysis of electronic device performance in various condition (Izuka & Fukuma, 1990).

Because of high mobility and high saturation velocity, InP has become an attractive material for electronic devices of superior performance among the III-phosphates semiconductors (Besikci *et al*., 2000). Therefore study of the electron transport in group III-phosphates is necessary. GaP possesses an indirect band gap of 0.6 eV at room temperature whereas InP and $Ga_{0.5}In_{0.5}P$ have a direct band gap about 1.8 eV and 1.5 eV, respectively (Bhuiyam et al., 2003).

In this article, the transport properties of bulk group III-phosphates in the temperature range from 300 to 600 K and in the applied electric field range from 0 to 500 kV/cm will be discussed (Martienssen & Warlimont, 2005). Simple, analytic expressions for the temperature and ionized impurity concentration dependences of high-field drift velocity are then proposed for incorporation into the group III-phosphates (Vurgaftman & Meyer, 2001). High-field transport properties in these materials are dominated by band structure effects, i.e, electron transfer to satellite valleys of the conduction band, which lead to a peak and a subsequent decrease in the drift velocity with increasing electric field (Arabshahi *et al*., 2008). Here, the temperature dependence of this phenomenon is examined and the drift velocity peak is characterized in terms of an analytic expression.

Details of the conduction band parameters and the employed simulation model are presented below, and results for simulation carriedout are also interpreted.

Simulation model

An ensemble Monte Carlo simulation has been used to investigate the electron transports in bulk semiconductors. This program simulated the trajectories of ten thousand quasi-particles as they move through the material under the influence of external forces and subject to random scattering events.

In order to calculate the electron drift velocity for large electric fields, consideration of conduction band satellite valleys is necessary (Jacoboni & Reggiani, 1983). One of the main inputs of the model is the energy band structure. The first-principles band structure of InP and $Ga_{0.5}In_{0.5}P$ predicts a direct band gap located at the Γ point and lowest energy conduction band satellite valleys at the X point and at the L point. In our Monte Carlo simulation, the Γ valley, the three equivalent X valleys, and the four equivalent L valleys were represented by spherical, non-parabolic, analytical effective mass expressions of the following form (Foutz *et al*., 1997; Albrecht *et al*., 1998),

$$E(k)[1+\alpha_i E(k)]=\frac{\hbar^2 k^2}{2m^*} \qquad (1)$$

Table 1. Important band parameters used in our simulation for GaP, InP and $Ga_{0.5}In_{0.5}P$

	Valley	Egap(eV)	m*	Nonparabolicity (eV^{-1})
GaP	Γ	2.24	0.3	0.2
	L	2.76	0.64	0.06
	X	2.0	0.17	0.15
InP	Γ	1.35	0.073	0.7
	L	0.6	0.3	0.5
	X	0.75	0.6	0.15
$Ga_{0.5}In_{0.5}P$	Γ	1.92	0.105	0.45
	L	0.125	0.242	0.001
	X	0.217	0.61	0.069

where m^* is effective mass at the band edge and α_i is the non-parabolic coefficient of the i-th valley (Bhapkar & Shur, 1997). Non-parabolic coefficients are obtained according to the Kane model (Kane, 1957) as

$$\alpha_i=\frac{1}{E_g}\left[1-\frac{2m^*}{m_0}\right]\left[1-\frac{E_g\Delta}{3(E_g+\Delta)(E_g+2\Delta/3)}\right] \qquad (2)$$

where Eg is the band-gap energy and Δ is the spin-orbit spilling. The band structure and material parameters necessary for calculating the scattering probabilities used

Indian Journal of Science and Technology Vol.2 No. 10 (Oct 2009) ISSN: 0974- 6846

in the present Monte Carlo simulation are given in Table 1 and 2.

The Monte Carlo model includes polar optical, acoustic phonon, ionized impurity and non-polar inter-valley phonon scattering which are the most important mechanisms that affect on the electron motion in the material (Newman et al., 1989).

Table 2.Material parameter selections for GaP, InP, and $Ga_{0.5}In_{0.5}P$

	GaP	InP	$Ga_{0.5}In_{0.5}P$
Density ρ(kgm^{-3})	4138	4810	4470
Longitudinal sound velocity vs(ms^{-1})	5850	5300	4330
Low-frequency dielectric constant ε_0	11.1	12.4	11.75
High-frequency dielectric constant ε_∞	9.11	9.55	9.34
Acoustic deformation potential D(eV)	3.1	8.3	7.2
Polar optical phonon energy (eV)	0.051	0.06	0.046
Energy gap (eV)	2.24	1.35	0.217
Intervalley deformation potentials ($10^7 eVm^{-1}$)	1	1	1
Intervalley phonon energies (meV)	51	29	10

Calculation results

Average electron energy as function of applied electric field is depicted in Fig.1 for temperatures up to 600K. Many aspect of electron behavior which has influenced by an external electric field, can be explained by it. It is clear that initially energy curves demonstrate a higher monotonic increase along with increasing external field. Thereafter, the energy increase only becomes slow with increasing of electric field. This feature is due to the electron transfer from the Γ valley to L and X valleys. The mean energy initial rise is due to the dominant contribution of the acoustic scattering mechanism until it reaches to a certain threshold value about 10, 100 and 2 kV/cm for InP, GaP and $Ga_{0.50}In_{0.50}P$, respectively. This increase is due to the quasi-elastic nature of the acoustic scattering and ionized impurity scattering (Jacoboni & Lugli, 1989). With increasing electric field more than the threshold fielded, the electrons have not enough energy to make the inter-valley scattering. Beyond this value, the optical scattering mechanisms play a drastic role rather than acoustic and ionized impurity scattering. Since this process is inelastic, electron energy curves have sensitive variation in its slope; in fact it does not increase as fast as increasing in initial fields.

Fig. 1. Calculated electron energy in bulk InP, GaP and $Ga_{0.5}In_{0.5}P$ as a function of applied electric field at various lattice temperatures and assuming a donor concentration of 10^{16} cm^{-3}.

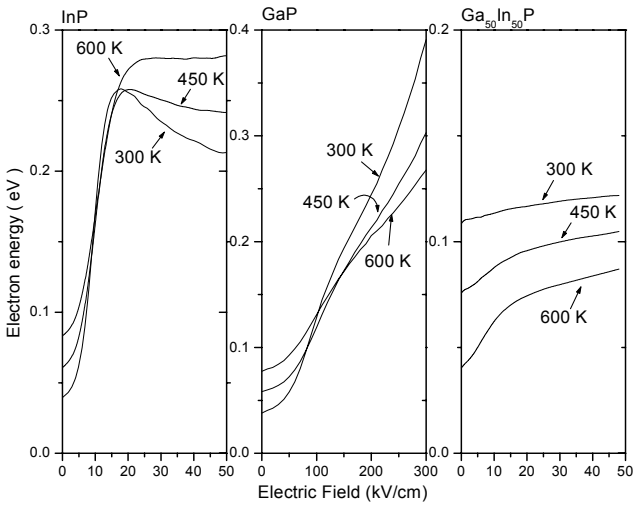

Fig.2 shows the velocity-field characteristic in bulk InP, GaP and $Ga_{0.5}In_{0.5}P$ at room temperature and with a background doping concentration of 10^{16} cm^{-3}. As can be seen, velocity-field characteristic exhibit a peak for InP and $Ga_{0.5}In_{0.5}P$ at about 2.3×10^5 and 1×10^5 ms^{-1}, respectively. The velocity-field curves typically present a decrease of the electron velocity, when the electric fields increase above the threshold value. This effect is due to the transfer of electrons from central Γ valley with low energy state and high mobility to higher valley with high energy state and low mobility. GaP has an indirect band gap and at lower electric fields, so electrons occupied X satellite valley at first. Hence, it is expected that its velocity-field curves does not have a peak. At higher electric field, inter-valley optical phonon emission dominates causing the drift velocity to saturate at around 0.6×10^5 ms^{-1}. Also we present experimental result for velocity-field characteristic of GaAs and InP in room temperatures. It is seen that our simulated results are in fair agreement with other results (Ridley, 1993).

Fig. 3 shows the calculated electron drift velocity as a function of electric field strength for temperatures of 300, 450 and 600 K. The decrease in drift mobility with temperature at low fields is due to increased intra-valley polar optical phonon scattering whereas the decrease in velocity at higher fields is due to increased intra and inter-valley scattering.

It can be seen from the Fig.3 that the peak velocity also decreases and moves to higher electric field as the temperature is increased. This is due to the general increase of total scattering rate with temperature, which suppresses the electron energy and reduces the population of the satellite valleys. This latter effect is apparent from the fact that the electron population in the Γ valley increases with temperature as shown in Fig. 4.

The importance of electron inter-valley transfer at high electric fields can be clearly seen in Fig. 4. In this figure the electron valley occupancy ratio for different materials is plotted. It is obvious that the inclusion of satellite valleys in the simulations is important. Significant electron transfer to the upper valleys only begins to occur, when the field strength is very close to the threshold value. Electrons, which are near a valley minimum, have small kinetic energies; therefore they have strongly scattered. It is apparent that inter-valley transfer is substantially larger in InP over the range of applied electric fields shown, due to the combined effect of a lower Γ effective mass, lower satellite valley separation energy, and slightly lower

Indian Journal of Science and Technology Vol.2 No. 10 (Oct 2009) ISSN: 0974- 6846

phonon scattering rate within the Γ valley. As can be seen, lowest valleys in conduction band in GaP are locate at *X* Point then electrons scattered to next lowest energy satellite valleys (Γ and *L* valleys) with increase of electric field.

Fig. 2. Calculated steady-state electron drift velocity in bulk InP, GaP and $Ga_{0.5}In_{0.5}P$ using non-parabolic band models in comparison with GaAs material and experimental measurements of Brennan et al., 1983

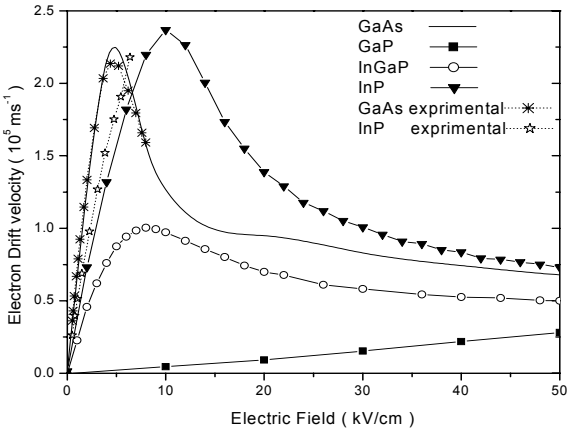

Fig.5 shows how the velocity-field characteristic of InP, $Ga_{0.5}In_{0.5}P$ and GaP materials change with impurity concentration at 300 K. It is clear that with increasing donor concentration, there are reduction in the average peak drift velocity and the threshold field because of increasing scattering rate events. As revealed by the results, the trend expected from increased ionized impurity scattering is in good general agreement with recent calculations by other investigations (Brennan *et al.*, 1983).

Conclusion

Electron transport at different temperatures in bulk GaP, InP and $Ga_{0.5}In_{0.5}P$ have been simulated using an ensemble Monte Carlo simulation. Using valley models to describe the electronic bandstructure, calculated velocity-field characteristics show that the inter-valley transitions in high electric fields play an important role in these materials. The inter-valley transitions lead to a large negative differential conductance. We have also shown that impurity concentration does not effect the electron transport properties in GaP semiconductor; therefore, GaP devices are expected be more tolerant to self-heating and high ambient temperature device modeling.

Fig. 3. Calculated electron steady-state drift velocity in bulk InP, GaP and $Ga_{0.5}In_{0.5}P$ as a function of applied electric field at various lattice temperatures and assuming a donor concentration of 10^{16} cm^{-3}. The peak drift velocity decreases while the threshold field increases by the same percent as the lattice temperature increases from 300 to 600 K.

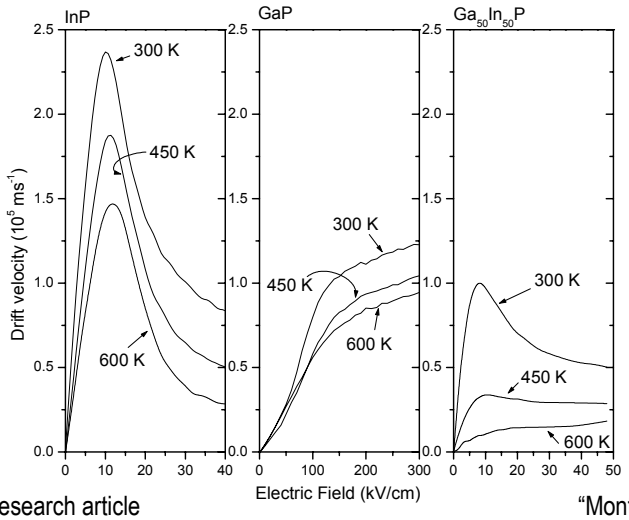

References

1. Albrecht JD, Wang RP, Ruden PP and Brennan KF (1998) Monte Carlo simulation of GaN in zincblende and wurtzite structures. *J. Appl.Phys*. 83, 2185-2190.
2. Arabshahi H, Khalvati MR and Rezaee Rokn-Abadi M (2008) Comparison of steady state and transient electron transport in InAs, InP and GaAs. *Modern Phys.Lett.B*, 22 (17), 1695-1702.
3. Arabshahi H, Khalvati MR and Rezaee Rokn-Abadi M (2008) Monte Carlo modeling of hot electron transport in bulk AlAs, AlGaAs and GaAs at room temperature. *Modern Phys.Lett.B*, 22 (18), 1777-1784.
4. Besikci B, Bakir M and Tanatar U (2000) Hot electron simulation devices. *J. Appl. Phys*. 88 (3) 1243-1247.
5. Bhapkar U V and Shur M S (1997) Ensemble Monte Carlo study of electron transport in wurtzite InN. *J. Appl. Phys.* 82, 1649-1654.
6. Bhuiyam S, Senoh M and Mukai T (2003) Comparison of steady state and transient electron *Appl. Phys. Lett*. 62, 2390-2395.
7. Brennan K, Hess K, Tang JY and Iafrate GT (1983) High field electron transport properties. *IEEE Trans.Electron Devices*, 30, 1750-1755.
8. Fischetti MV and Laux SE (1991) Low field electron mobility in GaN. *IEEE Trans.Electron Devices*, 38, 650-655.
9. Foutz BE, Eastman LE, Bhapkar UV and Shur M (1997) Full band Monte Carlo simulation of Zincblende GaN MESFET's including realistic impact ionization rates. *Appl. Phys. Lett.* 70, 2849-2854.
10. Ghani B, Hashimoto A and Yamamoto A (2003) High temperature characteristics of AlGaN/GaN modulation doped field-effect transistors. *J. Appl. Phys.* 94, 2779-2783.
11. Izuka J and Fukuma M (1990) Full-band polar optical phonon scattering analysis and negative differential conductivity in wurtzite GaN. *Solid-State Electron*, 3, 27-33.
12. Jacoboni J and Lugli P (1989) The Monte Carlo method for semiconductor and device simulation. Springer-Verlag.
13. Jacoboni J and Reggiani L (1983) The Monte Carlo simulation of Semiconductor and Devices. *Reviews of Modern Phys.* 55 (3) 665-663.
14. Kane EO (1957) Band structure calculation in group

III and IV materials. *J.Phys.Chem. Solids.* 1, 249-253.
15. Martienssen M and Warlimont H (2005) Springer

Fig. 4. Valley occupancy ratio of the central and satellite valleys in bulk InP, GaP and $Ga_{0.5}In_{0.5}P$ as a function of applied electric field using the non-parabolic band model at different temperatures up to 600 K.

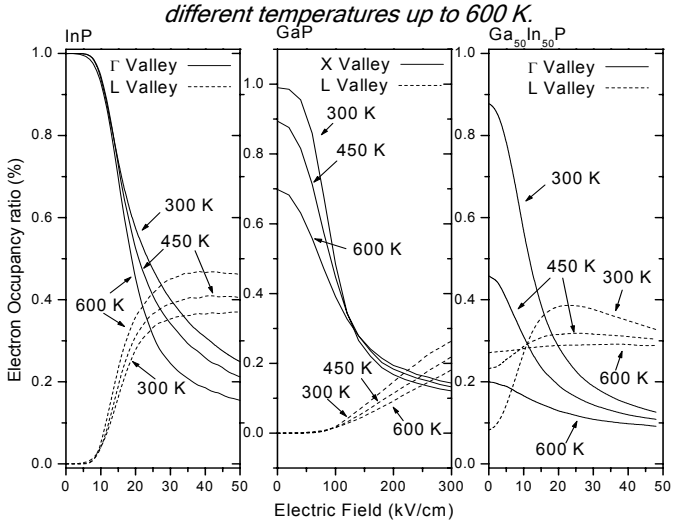

hand book of condensed Matter and Materials Data, Springer.
16. Newman N, Schilfgaarde V, Kendelewicz T and Spicer WE (1989) GaN based transistor for high power applications. *Mater. Res. Soc. Symp. Proc*. 21 54-59.
17. Ridley BK (1993) Quantum processes in semiconductors. Clarendon Press. Oxford.
18. Vurgaftman I and Meyer JI (2001) A review for GaN based devices. *J. Appl. Phys.* 89 (11) 887-889.
19. Yu Y and Cardona M (2001) Fundamentals of Semiconductors. 3rd ed., Springer, Berlin, Heidelberg.

Fig .5. Calculated electron steady-state drift velocity in bulk InP, GaP and $Ga_{0.5}In_{0.5}P$ as a function of applied electric field at various donor concentration up to 10^{18} cm^{-3} at room temperature. The peak drift velocity decreases due to increasing scattering rate